Advances in Technology Innovation, vol. 9, no. 4, 2024, pp. 287-300

Performance Evaluation of Neural Network Models for Autism Detection Using EEG Data

Nazmul Hasan[1,*], Priyasha Paul[2], Manisha Jitendra Nene[1]

[1]School of Computer Engineering and Mathematical Sciences, Defence Institute of Advanced Technology, Pune, India

[2]Department of Biosciences, Manipal University Jaipur, Jaipur, India

Received 01 July 2024; received in revised form 31 July 2024; accepted 02 August 2024

DOI: https://doi.org/10.46604/aiti.2024.13951

Abstract

This study aims to leverage a promising avenue for the precise and early detection of Autism. Autism is a multifaceted neurodevelopmental condition marked by challenges in social interaction, communication, and repetitive behaviors. Traditional diagnosis relies on time-consuming behavioral assessments, necessitating reliable and non-intrusive biomarkers for early and accurate detection. This paper analyzes eleven linear and non-linear features across time and frequency domains from an EEG dataset. Four neural network models, such as convolutional neural network (CNN), deep neural network (DNN), long short-term memory (LSTM), and a custom neural network are employed for classification. The CNN achieves the lowest accuracy at 89.02%, while the custom neural network reaches the highest accuracy at 94.02%, and the DNN and LSTM achieve 91.98% and 93.83% accuracy, respectively. Other metrics such as precision, recall, specificity, and F1-score, are also evaluated. This research underscores the efficacy of neural network in detecting Autism, advancing diagnostic tools.

Keywords: Autism, detection, EEG, machine learning, neural network

1. Introduction

Autism spectrum disorder (ASD) is a complex neurodevelopmental condition characterized by a spectrum of challenges, including difficulties in communication, response, attention, social behavior, and repetitive activities [1-7]. Beyond these primary symptoms, individuals with ASD exhibit atypical neural activity patterns [8]. Diagnosing Autism presents complexity owing to its diverse symptoms and their varying degrees among individuals [9]. Early detection and intervention are crucial for optimizing outcomes and providing appropriate support for individuals with ASD [10]. The present diagnostic approach for ASD predominantly depends on subjective and time-consuming behavioral assessments [11].

The recent research explores diverse physiological markers such as eye tracking, functional magnetic resonance imaging (fMRI), and gait movements for identifying patterns to facilitate more accurate early diagnosis of Autism and improve intervention techniques [12-14]. Another promising avenue in this pursuit involves analyzing electroencephalogram (EEG) data [15]. EEG signals capture subtle electrical fluctuations in the brain, presenting valuable information about neural responses to various stimuli [16]. EEG data also provides insights into brain function and connectivity, offering the opportunity to explore neural processes [17]. The recognition of atypical neural activity in individuals with Autism has interest in utilizing EEG data as a potential biomarker for ASD [18]. Recent advancements in the machine learning (ML) approach for EEG analysis have shown promise in addressing this need [19-21]. Several studies have explored the use of ML techniques to analyze EEG data for ASD detection [22-24]. However, there is still a need for more comprehensive studies that explore a broader range of neural network (NN) models and feature selections.

* Corresponding author. E-mail address: nazmulcse10@gmail.com

English language proofreader: Yen-Chun Hsieh

This study aims to leverage this promising avenue by exploring eleven distinct linear and non-linear features across time and frequency domains from EEG data. By employing four NN models such as a convolutional neural network (CNN), deep neural network (DNN), long short-term memory (LSTM), and a custom NN—this research seeks to enhance the precision and early detection of Autism. The performance of these models is evaluated using accuracy, precision, recall, specificity, and F1-score metrics.

In this study, ML-based NN is employed to classify ASD using EEG signal analysis. The primary objective is to implement and evaluate the different ML-based NN models, including deep and custom-designed NNs, for accurately identifying patterns in EEG data that are indicative of ASD. By focusing solely on EEG data, the study of this paper provides a comprehensive understanding of the potential of EEG-based biomarkers for Autism detection. This paper represents a significant contribution by presenting highly accurate models for identifying ASD solely through EEG signal analysis. The outcomes of this research offer potential tools for early detection of Autism, addressing a critical need in the field. Furthermore, this analysis enhances the understanding of the neural characteristics associated with ASD and lays the groundwork for the development of targeted interventions and therapies.

The subsequent sections of this paper are structured as follows: Section 2 provides an overview of related research works in the field of EEG-based Autism detection. Section 3 presents the methodology for the study of this paper, including the dataset and extracted features. Section 4 presents the NN models employed in this study. Section 5 presents the results of this study. Finally, Section 6 provides a discussion and conclusion on the findings of this study.

2. Related Works

Extensive research has been dedicated to the analysis of EEG signals for Autism detection. Some of the key findings in current research on Autism detection through EEG signals using ML are highlighted in this section. Table 1 provides a comprehensive summary of research on EEG analysis for Autism detection using various ML approaches.

Table 1 Highlights and comparison of the existing research works

Reference	Publication year	ML approaches	Extracted features	Participants ASD/TD	Classification accuracy
Heunis et al. [19]	2018	LDA, MLP, and SVM	RQA	16/46	92.9%
Haputhanthri et al. [20]	2019	LR, SVM, NB, and RF	Statistical features (mean and standard deviation)	10/5	93%
Abdolzadegan et al. [21]	2020	KNN	Power spectrum, wavelet transform, FFT, fractal dimension, correlation dimension, Lyapunov exponent, entropy, detrended fluctuation analysis, synchronization likelihood	34/11	72.77%
		SVM			90.57%
Radhakrishnan et al. [22]	2021	DNN	Automatic feature extraction and classification	10/10	81%
Garcés et al. [23]	2022	Linear support vector classifier (SVC), Elastic Net LR, radial basis function SVC	Power spectrum and functional connectivity	212/199	56% to 64%
Peketi and Dhok [24]	2023	EBT, SVM with a fine Gaussian kernel, and artificial neural network (ANN)	Linear and non-linear features across time and frequency domains	15/0	91.12%
This study	2023	CNN	Linear and non-linear features across time and frequency domains	13/4	89.02%
		DNN			91.98%
		LSTM			93.83%
		Custom NN			94.02%

The existing studies employed diverse approaches including linear discriminant analysis (LDA), multi-layer perceptron (MLP), support vector machine (SVM), logistic regression (LR), naive Bayes (NB), random forest (RF), K-nearest neighbor (KNN), DNN, and ensemble bagged tree (EBT) [19-24]. Feature extraction techniques encompassed recurrence quantification

analysis (RQA), statistical features, power spectrum analysis, wavelet transforms, fast Fourier transform (FFT), fractal dimension, correlation dimension, Lyapunov exponent, entropy, detrended fluctuation analysis, synchronization likelihood, linear and non-linear features across time and frequency domains [19-24]. Classification accuracy across these studies ranged from 56% to 93%, showcasing the potential of ML in accurately discerning ASD patterns from typically developing (TD) individuals, thereby contributing to the development of effective diagnostic tools and interventions [19-24].

This study is distinct from earlier research in its eleven time and frequency domain features selection in distinguishing between EEG patterns associated with TD and individuals with ASD. This elevated level of accuracy highlights the study's importance as it offers a more precise and dependable tool for the early detection of Autism. These results hold significant promise for contributing substantially to both Autism research and clinical applications.

3. Methodology

This section details the approach taken in this research to analyze EEG data from children diagnosed with ASD and TD. This study utilizes the global datasets for Autism disorder, which includes high-quality EEG recordings obtained under controlled conditions, ensuring reliability in the data. A detailed feature extraction process is conducted to derive both time-domain and frequency-domain characteristics, providing a comprehensive understanding of the underlying neural patterns. By integrating these features, the study aims to effectively differentiate between the two groups using ML models.

3.1. Dataset overview

The dataset utilized in this research, known as the global datasets for Autism disorder, is obtained from the brain-computer interface (BCI) group at King Abdulaziz University (KAU) with the necessary permissions for this study [25]. Comprising EEG recordings from two distinct groups, the dataset includes thirteen boys, aged 10 to 16 years, diagnosed with ASD in the first group. The second group consists of four TD boys, aged 9 to 16 years.

The EEG signals were recorded during participants' relaxed states to ensure artifact-free data, using the g.tec EEGcap, 16 Ag/AgCl electrodes, g.tec GAMMAbox, g.tec USBamp, and BCI2000 system. The EEG data were acquired from 16 electrodes, including FP1, FP2, F7, F3, Fz, F4, F8, T3, C4, Cz, C3, T5, Pz, O1, Oz, and O2 according to the 10-20 international system. The anterior frontal Z (AFz) electrode served as ground (GND), while the right ear lobe was used as reference (REF). The recorded data were filtered using a bandpass filter within the frequency range of 0.1-60 Hz and a notch filter at 60 Hz, subsequently digitized at 256 Hz. This dataset is chosen for its comprehensive and controlled acquisition method, providing high-quality, reliable EEG data crucial for distinguishing between ASD and TD children.

Initially, the data is segmented into fixed-length epochs, and any null values are removed to ensure accurate feature extraction. The total number of epochs in the dataset for initial and after preprocessing are 5437 and 5402 respectively, and their distribution between the training and testing sets are 4321 and 1081 respectively. This information is crucial for understanding the dataset's overall size and composition, which is important for ensuring the accuracy and generalizability of any NN models trained on it. Additionally, understanding the distribution of epochs in the training and testing sets helps identify any potential biases or imbalances in the data.

3.2. Extracted features

The study explores eleven distinct linear and non-linear features across time and frequency domains from an EEG dataset utilizing ML-based NN models. These features encompass a variety of statistical, spectral, and signal processing measures, contributing to the analysis and interpretation of EEG data. Out of eleven features, six are time domain and five are frequency domain features. The explored features are discussed below.

Mean: The mean is a statistical measure that represents the average value of a set of numbers or data points. The mean is computed mathematically by adding all of the values in the dataset and dividing the total number of data points. Having a dataset with n data points, denoted by $x_1, x_2, x_3, ..., x_n$, the mean (μ) can be calculated as:

$$\mu = \frac{x_1 + x_2 + x_3 + \ldots + x_n}{n} \tag{1}$$

Quantile: Based on a collection of input features, quantile ML involves calculating the conditional quantiles of a target variable. The purpose of quantile is to discover a mathematical function that links the quantiles of the target variable y with the input features x. Let's denote the conditional quantile of y at a given percentile q as $Q_q(y|x)$. The quantile regression minimizes the weighted absolute loss function, as shown in the following equation. Given the input characteristics x, $f(x)$ here denotes the expected quantile of y. Based on the specified quantile level q, the loss function penalizes the errors.

$$L_q\left(y, f(x)\right) = \left(1-q\right) \times \max\left(0, y - f(x)\right) + q \times \max\left(0, f(x) - y\right) \tag{2}$$

SVD entropy: The singular value decomposition (SVD) and Shannon entropy are used to quantify the randomness of a dataset. It gives a measurement of the dataset's level of uncertainty. The Shannon entropy mathematical formula is used to determine the SVD entropy. The average amount of information or uncertainty in a dataset is measured by Shannon entropy, as shown below.

$$Entropy = -\sum\left(p \times \log_2(p)\right) \tag{3}$$

Here, p denotes the probability distribution of the singular values and $\sum$ denotes the sum.

Peak-to-peak amplitude (*PPA*): PPA is an ML feature that measures the difference between the maximum and minimum values of a signal within a given time interval, as shown in the following equation. It is commonly used in various signal-processing applications, including audio and vibration analysis.

$$PPA = \max\left(x\right) - \min\left(x\right) \tag{4}$$

The $\max(x)$ represents the maximum value of the signal within the specified time interval. The $\min(x)$ represents the minimum value of the signal within the specified time interval.

Energy frequency bands: Energy frequency bands record data on the signal's energy distribution across several frequency bands. Considering a signal $x(t)$ and applying the Fourier transform to obtain its frequency-domain representation $x(f)$, where f represents frequency. The frequency range is divided into bands, such as the low-frequency, mid-frequency, and high-frequency bands. By adding the squared magnitudes of the Fourier coefficients within the respective frequency range, it computes the energy inside each band. The energy E_i within a frequency band i is computed, as shown below.

$$E_i = \sum\left|x(f)\right|^2 \tag{5}$$

Here, f is the frequency range of band i.

Spectral edge frequency (*SEF*): This characteristic in machine learning describes the distribution of frequencies in a signal, as shown in the following equation. It demonstrates how much high-frequency content is in a signal, information that can be helpful in a variety of applications, including audio and image processing.

$$SEF = \frac{\int[0, f]\, f \times P(f)df}{\int[0, \propto]\, f \times P(f)df} \tag{6}$$

Here, $P(f)$ is the power spectral density (PSD) of the signal and f represents the frequency.

Standard deviation (*SD*): This metric quantifies the dispersion of the feature values around the mean. In ML, SD is frequently used as a feature engineering technique to assess a feature's importance in predictive models and capture its variability, as shown below.

$$SD = \sqrt{\frac{1}{N} \times \sum \left(x_i - \mu \right)^2} \tag{7}$$

Here, the dataset's total number of data points is N. Each distinct feature value is represented by the x_i. The μ represents the feature values' mean. The $\sum$ stands for the total of the squared disparities.

Hjorth mobility (*HM*): This parameter reveals the frequency content and signal variations. A signal with a greater mobility value denotes one with a higher frequency content or rate of change, whereas a signal with a lower mobility value denotes one with a lower frequency content or rate of change. It is determined using the three statistical measurements known as the Hjorth parameters that are deduced from the signal. Activity (A), mobility (M), and complexity (C) are the three Hjorth parameters, as shown below.

$$HM = \sqrt{\frac{M}{A}} \tag{8}$$

Spectral entropy (*SE*): A characteristic used in ML and signal processing to measure the spectral complexity or information content of a signal's frequency spectrum, as shown in the following equation. For SE, the signal's PSD, which depicts the signal's power distribution across several frequencies, is necessary. Methods like the Fourier transform or the periodogram are used to obtain the PSD.

$$SE = -\sum \left[P(f) \times \log_2 \left(P(f) \right) \right] \tag{9}$$

Here, the summation is done over the entire range of frequencies, and $P(f)$ indicates the normalized PSD at frequency f.

Skewness: Skewness is a statistical metric used in data analysis and ML to express the asymmetry from symmetry in a data distribution. It reveals details about the distribution's shape, including whether it is skewed left or right. A dataset's skewness is mathematically determined as the third standardized moment, as shown below.

$$Skewness = E\left[\left(\frac{x - \mu}{\sigma} \right)^3 \right] \tag{10}$$

Here, x is the data point, μ is the dataset mean, σ is its SD, and E stands for the anticipated value.

Kurtosis: Kurtosis is a statistical index used in data analysis and ML to describe the peak or flatness of a data distribution. It reveals details about the distribution's shape, including if it has thick tails or a denser center than a typical distribution. The fourth standardized moment is used to calculate a dataset's kurtosis, as shown below.

$$Kurtosis = E\left[\left(\frac{x - \mu}{\sigma} \right)^4 \right] \tag{11}$$

Time-domain and frequency-domain features are selected in this study for their complementary roles in capturing different aspects of EEG signals. Time-domain features (such as mean, SD, and HM) provide insights into the statistical and temporal characteristics of the EEG data, revealing patterns and variations over time. Frequency-domain features (such as SVD entropy, energy frequency bands, and SE) analyze the spectral content, identifying the distribution of signal power across various frequency bands, which is crucial for understanding the underlying neural oscillations and rhythmic activities. This combination ensures a comprehensive analysis, enhancing the ability to distinguish between ASD and TD children.

4. Neural Networks Employed for Autism Detection

The study utilizes EEG analysis to distinguish between ASD and TD children, employing four distinct NN models: CNN, DNN, LSTM, and a custom-designed NN model. The CNNs are chosen for their ability to capture spatial hierarchies in data, making them effective in extracting spatial features from EEG signals. The DNNs are included for their capacity to learn complex representations and intricate relationships within the high-dimensional EEG data. The LSTMs are selected due to their proficiency in learning temporal dependencies, which is crucial for analyzing sequential EEG data and capturing long-term patterns. Lastly, the custom-designed NN model is tailored specifically to the EEG dataset and classification task, allowing for the incorporation of domain-specific knowledge and fine-tuning for optimal performance. This combination of models leverages their respective strengths in spatial, complex, temporal, and customized feature extraction, enhancing the accuracy and reliability of distinguishing between ASD and TD children.

4.1. Convolutional neural network model

The CNN model (Fig. 1) for binary classification between TD and ASD using EEG data comprises the input data with a reshaped layer to a suitable shape for Conv1D layers, as follows.

$$X_{reshaped} = \text{Reshape}\left(X, batch\_size.i, c\right) \tag{12}$$

Here, i is input data and c is the number of channels after reshaping the data.

The Conv1D layers (Y_i) of the employed CNN model performed convolutions with kernels (W_i), and biases (b_i) followed by rectified linear unit (ReLU) activation, as follows.

$$Y_i = \text{ReLU}\left(W_i \times X_i + b_i\right) \tag{13}$$

Here, ReLU is defined in the following equation.

$$\text{ReLU}\left(x\right) = \begin{cases} 0, & if \ \ x < 0 \\ x, & if \ \ x \geq 0 \end{cases} \tag{14}$$

The MaxPooling1D layers reduce the spatial dimensions, as follows.

$$Z_i = \text{MaxPooling1D}\left(X_i, pool\_size\right) \tag{15}$$

The GlobalMaxPooling1D operation across the temporal dimension produces a vector output, as follows.

$$G = \text{GlobalMaxPooling1D}\left(x\right) \tag{16}$$

Dense layers perform fully connected operations with weights (W_l), biases (b_l), and activations. The Dense operation for a layer can be written as follows.

$$Y_i = \text{Activation}\left(W_l \times X_l + b_i\right) \tag{17}$$

Here, activation represents ReLU for hidden layers, and sigmoid for the output layer is shown below.

$$Sigmoid\left(x\right) = \frac{1}{1+e^{-x}} \tag{18}$$

The employed CNN model is compiled using the Adam optimizer and binary cross-entropy loss, monitoring accuracy as a metric. During training, the model learns training data for 50 epochs using a batch size of 60 and evaluates its performance on validation data. After training, the model is evaluated on test data, calculating the loss and accuracy metrics. Finally, predictions are generated using the trained model on the test data, producing predicted probabilities.

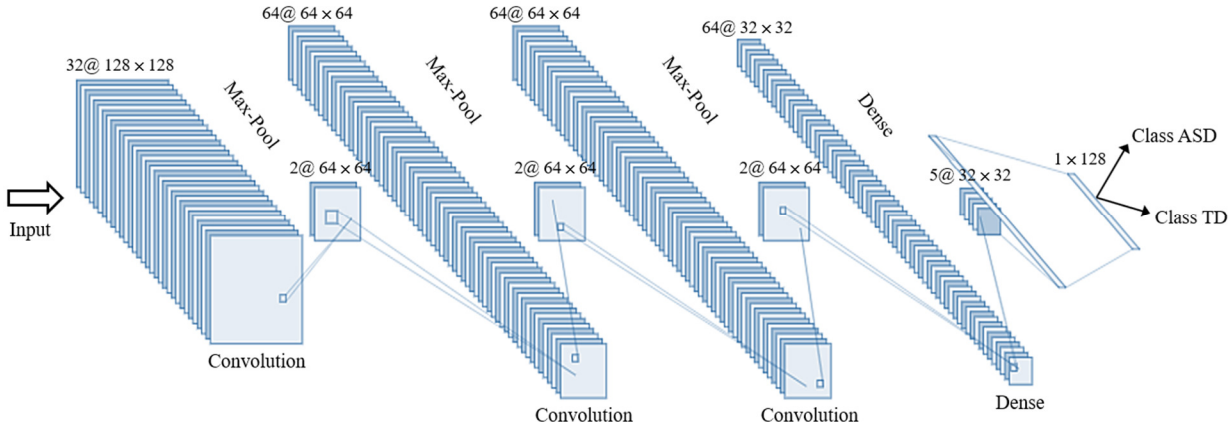

Fig. 1 Architecture of the CNN model employed in the study

4.2. *Deep neural network model*

The DNN model employed for the study (Fig. 2) comprises three Dense layers. The initial layer consists of 128 neurons and employs the ReLU activation function, as follows.

$$Output_1 = \mathrm{ReLU}\left(W_1 \times X + b_1\right) \tag{19}$$

Here, W_1 represents the weight matrix, X denotes the input data, b_1 is the bias term, and ReLU, represented by Eq. (13), represents the activation function.

The second Dense layer contains 64 neurons and also uses ReLU activation, as shown in the following equation. This layer introduces further non-linearity to capture complex patterns in the data.

$$Output_2 = \mathrm{ReLU}\left(W_2 \times Output_1 + b_2\right) \tag{20}$$

The final Dense layer consists of a single neuron using the sigmoid activation function, as shown below.

$$Output_{final} = \mathrm{Sigmoid}\left(W_3 \times Output_2 + b_3\right) \tag{21}$$

Similar to the employed CNN model, the DNN model in this study is compiled using the Adam optimizer and binary cross-entropy loss while monitoring accuracy. The training phase involves iterating over the training data for 50 epochs with a batch size of 60, utilizing validation data for validation purposes.

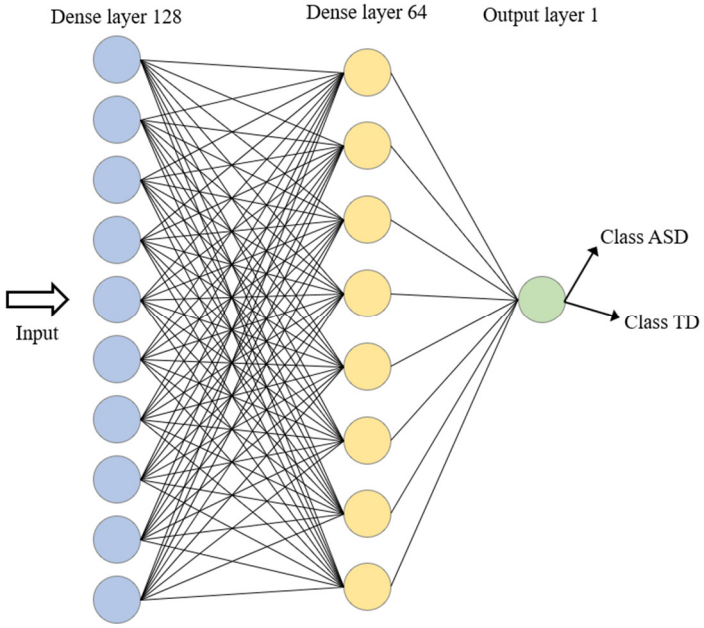

Fig. 2 Architecture of the DNN model employed in the study

4.3. Long short-term memory model

The employed LSTM model (Fig. 3) firstly reshapes the input data X_{train} and X_{test} for LSTM input compatibility. An LSTM layer is added to the sequential model. It consists of 64 neurons and utilizes the ReLU activation function. The LSTM cell operates as follows.

$$i_t = \sigma\left(W_i \times \left[h_{t-1}, x_t\right] + b_i\right) \tag{22}$$

$$f_t = \sigma\left(W_f \times \left[h_{t-1}, x_t\right] + b_f\right) \tag{23}$$

$$g_t = \tanh\left(W_g \times \left[h_{t-1}, x_t\right] + b_g\right) \tag{24}$$

$$O_t = \sigma\left(W_o \times \left[h_{t-1}, x_t\right] + b_o\right) \tag{25}$$

$$c_t = f_t \odot c_{t-1} + i_t \odot g_t \tag{26}$$

$$h_t = o_t \odot \tanh\left(c_t\right) \tag{27}$$

Here, i_t is input gate, f_t is forget gate, g_t cell gate, O_t is output gate, c_t is cell state, h_t is the hidden state, x_t input at timestep at t, the weight matrices are W_i, W_f, W_g, W_o and the bias terms are b_i, b_f, b_g, b_o.

The output layer is the Dense layer with a single neuron and sigmoid activation for binary classification. The model is compiled with the Adam optimizer and binary cross-entropy loss, as shown below.

$$Output_{final} = \text{Sigmoid}\left(W_{out} \times Output_{LSTM} + b_{out}\right) \tag{28}$$

$$L\left(Y_{true}, Y_{pred}\right) = -\frac{1}{N}\sum_{i=1}^{N}\left[y_{true} \times \log\left(y_{pred}\right) + \left(1 - Y_{true}\right) \times \log\left(1 - Y_{pred}\right)\right] \tag{29}$$

Here, N is the total number of data points.

During training, the model learns parameters by minimizing the defined loss function. The evaluation computes the loss (L) and accuracy metrics based on the test data. Predictions (y_{pred}) are generated using the trained LSTM model, providing probabilities for binary classification tasks.

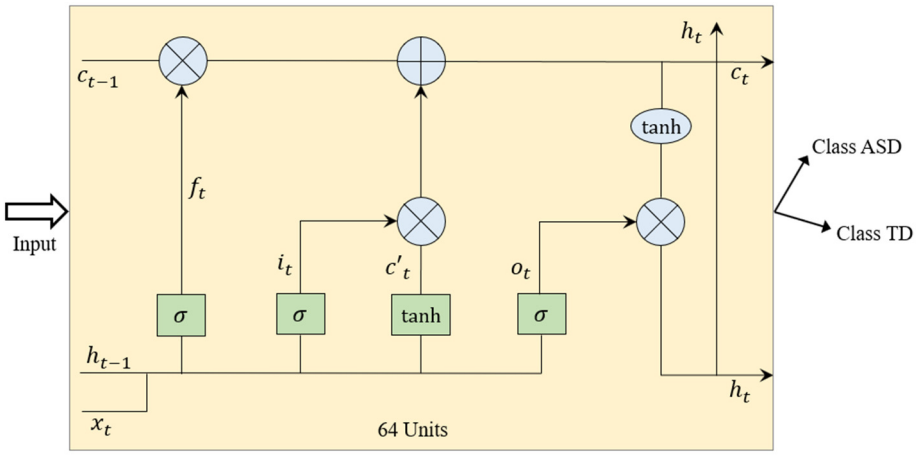

Fig. 3 Architecture of the LSTM model employed in the study

4.4. Custom neural network

The custom-designed NN for the study (Fig. 4) comprises several densely connected layers followed by batch normalization and dropout layers. The Dense layers, as shown in the following equations, contain 256, 128, 64, 32, and 16 neurons respectively, with ReLU activation functions, L2 regularization, and input dimensions matching the feature size of X_{train}.

$$z^i = w^i \times A^{(i-1)} + b^i \tag{30}$$

$$A^i = \mathrm{ReLU}\left(z^i\right) \tag{31}$$

Here, w^i is the weight, b^i is the bias and A^i is the activation output.

The batch normalization layers normalize the outputs of the previous layers to stabilize and improve the training process by reducing internal covariate shifts. Each dropout layer randomly sets a fraction of input units to zero during training to prevent overfitting. It aids in regularization by reducing interdependent learning among neurons. The model is compiled using the Adam optimizer with a learning rate of 0.001 and binary cross-entropy loss function, aiming to minimize the difference between predicted and true labels for binary classification tasks. After training, the model is evaluated using the test dataset to calculate the loss and accuracy metrics.

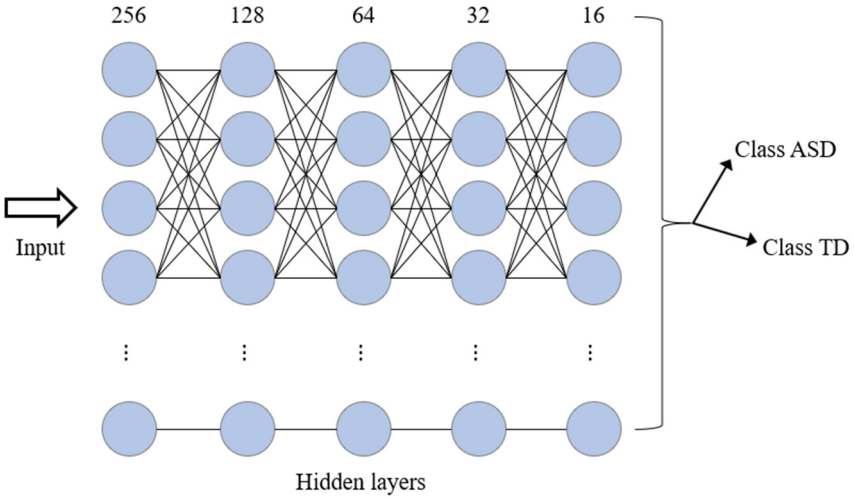

Fig. 4 Architecture of custom NN model employed in the study

4.5. *Evaluation metrics*

The parameters to evaluate the performance of this study are as follows. Here, true positive (TP), false positive (FP), true negative (TN), and false negative (FN) are defined.

Accuracy indicates the fraction of the total samples that were correctly classified by the classifier, as follows.

$$\text{Accuracy} = \frac{\text{TP} + \text{TN}}{\text{TP} + \text{TN} + \text{FP} + \text{FN}} \tag{32}$$

Recall measures the proportion of actual positives that were correctly identified by the model, as follows.

$$\text{Recall} = \frac{\text{TP}}{\text{TP} + \text{FN}} \tag{33}$$

Precision measures the proportion of correct positive predictions, as follows.

$$\text{Precision} = \frac{\text{TP}}{\text{TP} + \text{FP}} \tag{34}$$

Specificity measures the proportion of actual negatives that were correctly identified by the model, as follows.

$$\text{Specifity} = \frac{\text{TN}}{\text{TN} + \text{FP}} \tag{35}$$

The F1-score reflects the stability of the models by evaluating the balance between precision and recall, as follows.

$$\text{F1-score} = \frac{2\times(\text{Precision}\times\text{Recall})}{\text{Precision}+\text{Recall}} \tag{36}$$

The receiver operating characteristic (ROC) curve is a graphical tool used in ML to evaluate the performance of binary classifiers by plotting the TP rate against the FP rate at different thresholds.

5. Results

The t-distributed stochastic neighbor embedding (t-SNE) [26] figure shows the visualization of two classes (TD – 0.0, ASD – 1.0) in a two-dimensional space (Fig. 5). It demonstrates a partial separation of data points from both classes, indicating similarities and differences between the classes. While most points segregate into distinct clusters, some overlap occurs, suggesting shared features between individuals with ASD and TD individuals. The evaluation metrics for each of the employed NN models are presented in Table 2.

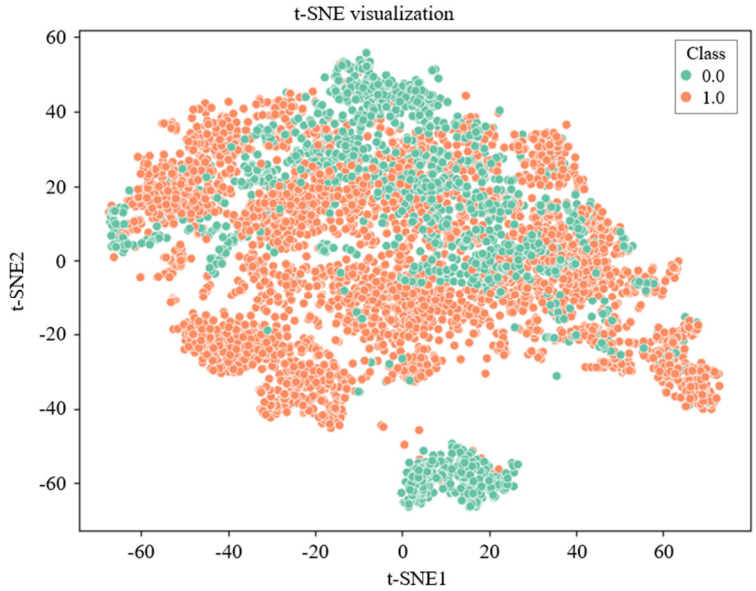

Fig. 5 Visualization of data points

Table 2 Evaluation metrics of the employed NN models

NN Model	Accuracy (%)	Precision (%)	Recall (%)	Specificity (%)	F1-score (%)
CNN	89.02	91.20	93.98	75.68	92.57
DNN	91.98	92.75	96.52	79.77	94.60
LSTM	93.83	95.08	96.52	86.60	95.80
Custom NN	94.02	95.85	95.94	88.86	95.90

The evaluation of performance metrics for distinguishing ASD and TD individuals using EEG data reveals significant insights across various NN models. Custom NN attained the highest accuracy at 94.02%, reflecting its superior classification ability due to its tailored architecture that effectively captures both spatial and temporal features. CNN had the lowest accuracy at 89.02%, indicating its limitations in handling the temporal dependencies in EEG data. In terms of precision, which measures the reliability of identifying ASD cases among the predicted positives, custom NN excelled at 95.85%, suggesting fewer FP due to its effective regularization techniques and optimized feature extraction. CNN had the lowest precision at 91.20%, indicating overfitting to some features while missing others. The recall indicates the ability to capture true ASD cases. The employed DNN, LSTM, and custom NN models have achieved high rates of 96.52%, showcasing their effectiveness in minimizing missed ASD cases. The LSTM's strength in handling sequential data contributes to its high recall, while custom NN's complex architecture enhances its sensitivity.

The CNN lagged in the recall at 93.98% due to its lower effectiveness in handling the temporal aspects of the data. Specificity, measuring the capability to correctly classify TD individuals, ranged from 75.68% for CNN to 88.86% for custom NN. The high specificity of custom NN suggests its proficiency in distinguishing non-ASD cases, likely due to its sophisticated design and regularization methods. CNN's lower specificity indicates a higher rate of FP, reflecting its challenges in accurately identifying TD cases. The F1-score, which balances precision and recall, was highest for custom NN at 95.90%, signifying its overall effectiveness and balanced performance. The LSTM also performed well with an F1-score of 95.80%, leveraging its architecture's strength in handling temporal data. The CNN shows the lowest F1-score at 92.57%, indicating its overall lower performance in balancing precision and recall.

These performance differences arise from the models' architectural strengths, data handling, regularization techniques, and feature extraction capabilities. Custom NN and LSTM demonstrate superior performance due to their sophisticated designs tailored for EEG data analysis, capturing complex patterns and temporal dependencies effectively. Fig. 6 shows the confusion matrices for the employed NN models which summarize the counts of TP, TN, FP, and FN predictions.

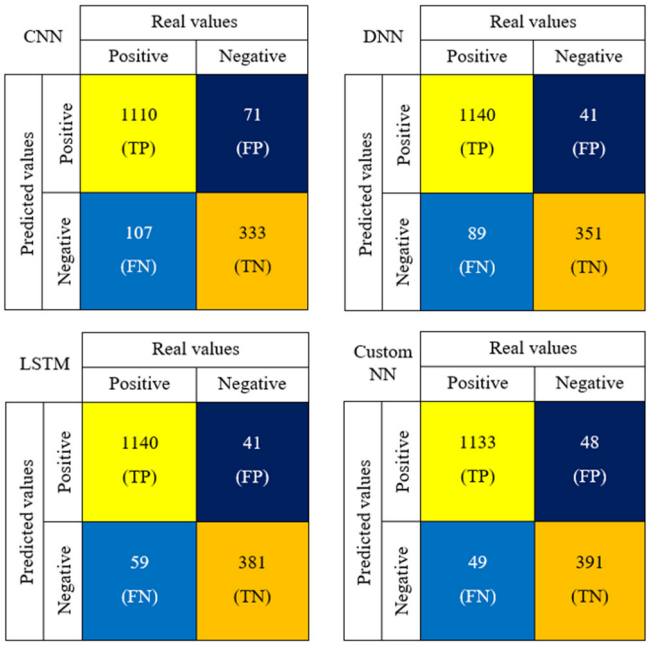

Fig. 6 Confusion matrices of the employed NN models

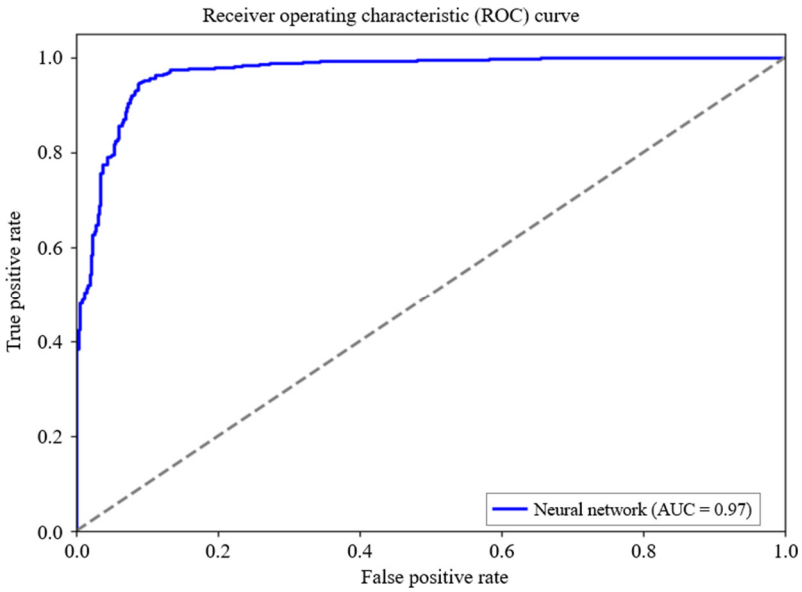

(a) ROC Curve for custom NN Model

Fig. 7 ROC curves for the employed NN models

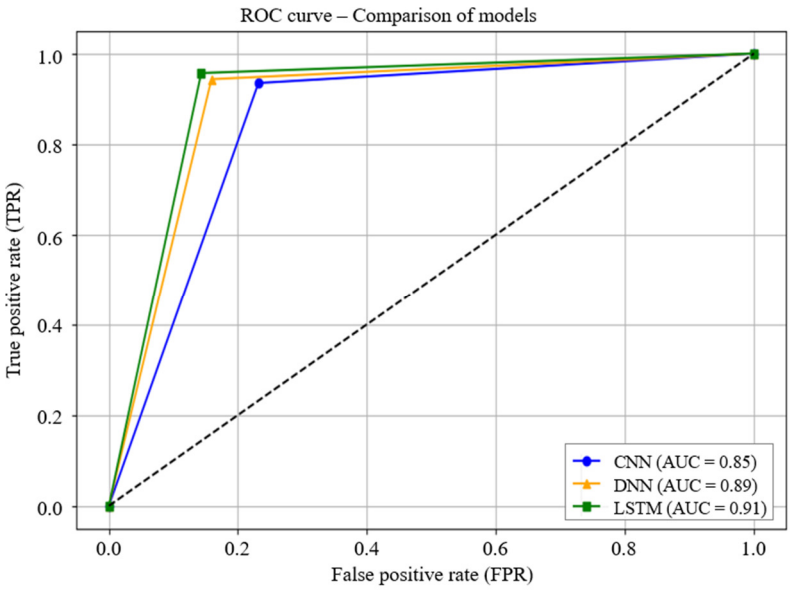

(b) ROC curve for CNN, DNN, LSTM

Fig. 7 ROC curves for the employed NN models (continued)

6. Discussion and Conclusion

The findings of this study underscore the potential of four NN models in the accurate classification of ASD using EEG data. Through a comprehensive evaluation of various NN models, including the standout custom NN, the study demonstrates notable advancements in distinguishing ASD cases from TD individuals. The analysis of accuracy, precision, recall, and specificity provides a well-rounded understanding of each model's strengths and limitations, with the custom NN exhibiting particularly strong performance. This highlights its potential for practical application in clinical settings, where early and accurate detection of ASD is crucial for effective intervention. The study significantly contributes to Autism research by showcasing the efficacy of NN models, particularly in offering non-intrusive diagnostic tools. The high accuracy of the custom NN model emphasizes the urgency and potential of early detection techniques in improving ASD diagnosis and intervention strategies. The varied performance across NN models reveals the potential for innovation in diagnostic tools and reinforces the importance of continued advancement in this area.

However, the study is not without its limitations. The reliance on a less diverse and relatively small dataset restricts the generalizability of the findings and the robustness of the developed models. This limitation impacts the models' performance in real-world scenarios, as the dataset does not fully represent the variability seen in ASD cases across different demographics and age groups. Future research should address these limitations by incorporating larger and more diverse datasets to enhance the generalizability and robustness of NN models. Additionally, exploring hybrid model frameworks that integrate various NN architectures could further improve diagnostic precision and clinical utility. Expanding the dataset and refining model frameworks will be crucial for advancing early ASD detection and developing more effective diagnostic tools, ultimately contributing to progress in Autism research and clinical practice.

Acknowledgment

The dataset (global datasets for autism disorder) used in this study is received from the brain-computer interface (BCI) group of King Abdulaziz University (KAU). Permission to use the dataset has been obtained for this study (https://malhaddad.kau.edu.sa/Pages-BCI-Datasets.aspx). The authors express their heartfelt thanks and gratitude to Dr. Mohammed J. Alhaddad from brain-computer interface (BCI) group of King Abdulaziz University (KAU) for providing and allowing the usage of the dataset.

Conflicts of Interest

The authors declare no conflict of interest.

Statement of Ethical Approval

For this type of study, statement of human rights is not required.

Statement of Informed Consent

For this type of study, informed consent is not required.

References

[1] N. Hasan and M. J. Nene, "Determinants of Technological Interventions for Children With Autism - A Systematic Review," Journal of Educational Computing Research, vol. 62, no. 1, pp. 250-289, March 2024.
[2] N. Hasan, M. N. Islam, and N. Choudhury, "Evaluation of an Interactive Computer-Enabled Tabletop Learning Tool for Children With Special Needs," Journal of Educational Computing Research, vol. 60, no. 8, pp. 2105-2137, January 2023.
[3] N. Hasan and M. J. Nene, "LEFA: Framework to Develop Learnability of Children with Autism," International Conference on Disruptive Technologies for Multi-Disciplinary Research and Applications (CENTCON), pp. 15-20, December 2022.
[4] N. Hasan and M. J. Nene, "MAPE: An Interactive Learning Model for the Children with ASD," Proceedings of International Conference on Communication and Computational Technologies, pp. 355-367, February 2022.
[5] N. Hasan and M. J. Nene, "ICT Based Learning Solutions for Children with ASD: A Requirement Engineering Study," International Journal of Special Education, vol. 37, no. 1, pp. 112-126, 2022.
[6] N. Hasan and M. J. Nene, "An Agent-Based Basic Educational Model for the Children with ASD Using Persuasive Technology," International Conference for Advancement in Technology (ICONAT), pp. 1-6, January 2022.
[7] N. Hasan and M. N. Islam, "Exploring the Design Considerations for Developing an Interactive Tabletop Learning Tool for Children with Autism Spectrum Disorder," Proceeding of the International Conference on Computer Networks, Big Data and IoT (ICCBI - 2019), pp. 834-844, December 2019.
[8] A. M. Gonçalves and P. Monteiro, "Autism Spectrum Disorder and Auditory Sensory Alterations: A Systematic Review on the Integrity of Cognitive and Neuronal Functions Related to Auditory Processing," Journal of Neural Transmission, vol. 130, no. 3, pp. 325-408, March 2023.
[9] Y. Hus and O. Segal, "Challenges Surrounding the Diagnosis of Autism in Children," Neuropsychiatric Disease and Treatment, vol. 17, pp. 3509-3529, 2021.
[10] R. C. Sheldrick, A. S. Carter, A. Eisenhower, T. I. Mackie, M. B. Cole, N. Hoch, et al., "Effectiveness of Screening in Early Intervention Settings to Improve Diagnosis of Autism and Reduce Health Disparities," JAMA Pediatrics, vol. 176, no. 3, pp. 262-269, March 2022.
[11] E. Helmy, A. Elnakib, Y. ElNakieb, M. Khudri, M. Abdelrahim, J. Yousaf, et al., "Role of Artificial Intelligence for Autism Diagnosis Using DTI and fMRI: A Survey," Biomedicines, vol. 11, no. 7, article no. 1858, July 2023.
[12] M. Parellada, A. Andreu-Bernabeu, M. Burdeus, A. San José Cáceres, E. Urbiola, L. L. Carpenter, et al., "In Search of Biomarkers to Guide Interventions in Autism Spectrum Disorder: A Systematic Review," American Journal of Psychiatry, vol. 180, no. 1, pp. 23-40, January 2023.
[13] J. Shan, Y. Gu, J. Zhang, X. Hu, H. Wu, T. Yuan, et al., "A Scoping Review of Physiological Biomarkers in Autism," Frontiers in Neuroscience, vol. 17, article no. 1269880, September 2023.
[14] C. Z. C. Hasan, R. Jailani, and N. M. Tahir, "Autism Spectrum Disorder and Normal Gait Classification Using Machine Learning Approach," Southeast Europe Journal of Soft Computing, vol. 12, no. 1, pp. 57-63, 2023.
[15] X. Geng, X. Fan, Y. Zhong, M. F. Casanova, E. M. Sokhadze, X. Li, et al., "Abnormalities of EEG Functional Connectivity and Effective Connectivity in Children with Autism Spectrum Disorder," Brain Sciences, vol. 13, no. 1, article no. 130, January 2023.
[16] F. Salto, C. Requena, P. Alvarez-Merino, V. Rodríguez, J. Poza, and R. Hornero, "Electrical Analysis of Logical Complexity: An Exploratory EEG Study of Logically Valid/Invalid Deducive Inference," Brain Informatics, vol. 10, no. 1, article no. 13, December 2023.

[17] G. Chiarion, L. Sparacino, Y. Antonacci, L. Faes, and L. Mesin, "Connectivity Analysis in EEG Data: A Tutorial Review of the State of the Art and Emerging Trends," Bioengineering, vol. 10, no. 3, article no. 372, March 2023.
[18] C. Clairmont, J. Wang, S. Tariq, H. T. Sherman, M. Zhao, and X. J. Kong, "The Value of Brain Imaging and Electrophysiological Testing for Early Screening of Autism Spectrum Disorder: A Systematic Review," Frontiers in Neuroscience, vol. 15, article no. 812946, 2021.
[19] T. Heunis, C. Aldrich, J. M. Peters, S. S. Jeste, M. Sahin, C. Scheffer, et al., "Recurrence Quantification Analysis of Resting State EEG Signals in Autism Spectrum Disorder – A Systematic Methodological Exploration of Technical and Demographic Confounders in the Search for Biomarkers," BMC Medicine, vol. 16, article no. 101, 2018.
[20] D. Haputhanthri, G. Brihadiswaran, S. Gunathilaka, D. Meedeniya, Y. Jayawardena, S. Jayarathna, et al., "An EEG Based Channel Optimized Classification Approach for Autism Spectrum Disorder," Moratuwa Engineering Research Conference, pp. 123-128, July 2019.
[21] D. Abdolzadegan, M. H. Moattar, and M. Ghoshuni, "A Robust Method for Early Diagnosis of Autism Spectrum Disorder From EEG Signals Based on Feature Selection and DBSCAN Method," Biocybernetics and Biomedical Engineering, vol. 40, no. 1, pp. 482-493, January-March 2020.
[22] M. Radhakrishnan, K. Ramamurthy, K. K. Choudhury, D. Won, and T. A. Manoharan, "Performance Analysis of Deep Learning Models for Detection of Autism Spectrum Disorder From EEG Signals," Traitement Du Signal, vol. 38, no. 3, pp. 853-863, June 2021.
[23] P. Garcés, S. Baumeister, L. Mason, C. H. Chatham, S. Holiga, J. Dukart, et al., "Resting State EEG Power Spectrum and Functional Connectivity in Autism: A Cross-Sectional Analysis," Molecular Autism, vol. 13, article no. 22, 2022.
[24] S. Peketi and S. B. Dhok, "Machine Learning Enabled P300 Classifier for Autism Spectrum Disorder Using Adaptive Signal Decomposition," Brain Sciences, vol. 13, no. 2, article no. 315, February 2023.
[25] "Global Datasets for Autism Disorder," https://malhaddad.kau.edu.sa/Pages-BCI-Datasets.aspx, June 03, 2023.
[26] R. Silva and P. Melo-Pinto, "t-SNE: A Study on Reducing the Dimensionality of Hyperspectral Data for the Regression Problem of Estimating Oenological Parameters," Artificial Intelligence in Agriculture, vol. 7, pp. 58-68, March 2023.